Diamond & Related Materials 152 (2025) 111978

Contents lists available at ScienceDirect

Diamond & Related Materials

journal homepage: www.elsevier.com/locate/diamond

Single crystal diamond polishing assisted by inductively coupled plasma etching

Jiarong Yu, Xinyue Liu, Rongbin Xu *, Daquan Yu *

School of Electronic Science and Engineering, Xiamen University, Xiamen 361005, Fujian, China

ARTICLE INFO

Keywords:
Single crystal diamond
Combination application
Inductively coupled plasma etching
Dynamic friction polishing

ABSTRACT

In order to achieve high efficiency and high quality polishing of single crystal diamond (SCD), a combined application method of inductively coupled plasma (ICP) etching and dynamic friction polishing (DFP) was developed. This study confirmed that a large amount of sp^2 C is generated on the single crystal diamond surface after processed by O_2 plasma, and then by DFP, a high flatness diamond surface can be obtained. By optimizing ICP etching and DFP parameters, Ra measured by atomic force microscope (AFM) at a scanning area of 10 μm*10 μm is as low as 0.185 nm. Moreover, X-ray photoelectron spectroscopy (XPS) and Raman spectroscopy were used to characterize the initial surface, plasma etched surface and polished surface of diamond samples. It can be concluded that this method can produce more amorphous carbon on the rough diamond surface, and amorphous carbon is easier to be removed by polishing, finally achieving a high flatness diamond surface. This study is of great significance for achieving high-level industrialization applications of diamond.

1. Introduction

With the development of the semiconductor industry, the demand for high-power electronic devices is increasing, and the traditional semiconductor materials such as silicon and germanium have been difficult to meet the actual demand. Therefore, wide band gap semiconductor materials such as silicon carbide, gallium nitride and diamond [1] have attracted much attention. Diamond, in particular, with its extreme band gap of 5.47 eV [2], is considered the ultimate semiconductor material. In addition, diamond also has the natural highest thermal conductivity of about 2200 W/m*k [3], the thermal expansion coefficient of as low as $0.8*10^{-6}\ k^{-1}$, as well as the scope from ultraviolet to far-infrared optics. The above excellent characteristics make it widely used in high power density thermal diffusers, diamond film coatings, diamond microwave windows, optical active Raman laser crystals, bipolar diamond electronic devices and so on [4–7]. The successful manufacture of synthetic diamond makes diamond obtain more advanced technology applications.

The above diamond applications require high-quality clean surfaces, however, for diamond materials, the hardness of 57–100 GPa [8] greatly increases the difficulty of processing [9]. Therefore, over the years, people have studied and designed a variety of processing methods for diamond polishing. Watanabe et al. [10] combined with chemical mechanical polishing (CMP) and ultraviolet-induced photochemical reaction. The oxidation is performed on the diamond surface under the action of local high temperature through ultraviolet light irradiation, and then removed it in the form of CO and CO_2 gas. Grodzinski [11] first prepared hot metal plates by using metal such as iron, nickel, manganese. Under the vacuum conditions carbon atoms will diffuse from the diamond surface to the thermal metal plate, so as to achieve thermal chemical polishing. Ollison et al. [12] combined chemical reaction with mechanical polishing by using chemical-assisted mechanical polishing (CAMPP) method. Under the action of load, the mechanical grinding of the metal polishing disc and the melting KNO_3/KOH caused the oxidation reaction of the diamond film at the same time, thereby achieving polishing to the diamond surface. Zhang et al. [13] adopted automatic high-precision high-speed three-dimensional movement (3DM)-DFP to carry out multi-dimensional movement on the diamond surface to avoid diamond surface scratches. The surface quality is significantly improved.

The various diamond polishing methods mentioned above have problems such as low polishing efficiency, complex processing technology and excessive experimental environment requirements. Therefore, for advanced technical diamond applications, it is not only necessary to reduce its operational difficulty and develop a fast, high-quality polishing process, but also to reduce its mechanical impact to

* Corresponding authors.
E-mail addresses: xurongbin@xmu.edu.cn (R. Xu), yudaquan@xmu.edu.cn (D. Yu).

https://doi.org/10.1016/j.diamond.2025.111978
Received 19 October 2024; Received in revised form 20 December 2024; Accepted 9 January 2025
Available online 10 January 2025

Table 1
Diverse ICP processes and related parameters.

Experimental group	Lower electrode power (W)	Upper electrode power (W)	Etching time (s)	Gas flow (sccm)
SCD1	50	300	120	50
SCD2	100	300	120	50
SCD3	50	500	120	50
SCD4	50	300	300	50

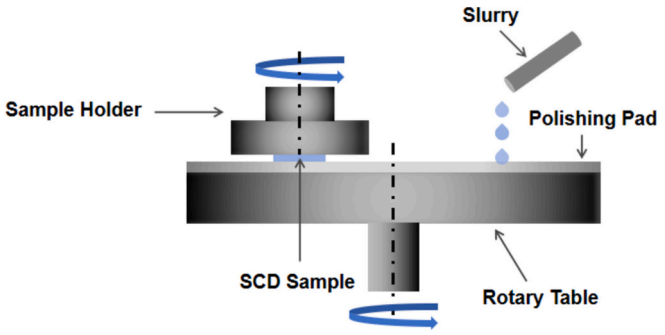

Fig. 1. Schematic diagram of DFP device.

avoid surface crystal damage. It had been reported that diamond treated by plasma is beneficial to its subsequent polishing [14]. Therefore, this study designed a combined process of inductively coupled plasma etching and dynamic friction polishing for single crystal diamond. The polished diamond samples were tested by AFM, Raman spectroscopy and XPS. The measurements show that the polished sample has a high smooth surface and the Ra value as low as 0.185 nm, and can attribute to the formation of amorphous carbon on rough diamond surface after ICP etching in oxygen atmosphere. This study provides a good solution for simplifying diamond polishing environment and improving diamond polishing quality.

2. Experimental methods

2.1. ICP etching

Inductively coupled plasma etching is the modification of diamond surface by plasma physical bombardment and chemical reaction [15]. To explore the impact of ICP experimental parameters on the polishing experiments of diamonds, different upper/lower electrode power and etching time were set up. Since diamond is a carbon-based material, oxygen was used as a reaction and etching gas. The experiment details are shown in Table. 1.

2.2. Dynamic friction polishing

Fig. 1 shows the device schematic diagram of DFP polishing experiment. Under the action of the load, the single crystal diamond sample and polishing plate and the abrasive in the polishing liquid rub each other, making the carbon atom structure on the surface is destroyed, and the diamond is transformed into the graphite phase under the action of local high temperature, and the amorphous carbon is further generated.

For the polishing experiment, the greater the hardness of the abrasive in the polishing liquid, the stronger the polishing pressure and mechanical action effect on the surface of the diamond sample. Diamond micro-powder is used in the abrasive in the polishing liquid. According to the size of the initial roughness of the diamond surface, the abrasive particle size is selected to be 4 μm. The polishing pad material used in the DFP polishing experiment is nubuck, the polishing speed is 45 rpm; the rotation speed of sample holder is 20 rpm; the polishing time is 8 h; the weight of the polishing vehicle is 2100 g, and it is equipped with four weighing blocks of 100 g each. Therefore, the total pressure exerted on the SCD sample is 25 N. Because the size of the sample is 0.7 cm*0.7 cm, the experiment is carried out under the parameter of 0.51 MPa with a polishing pressure.

To verify the effect of ICP etching and DFP polishing combination application for diamond surface polishing, a control group SCD5 without any etching treatment was used for polishing experiments.

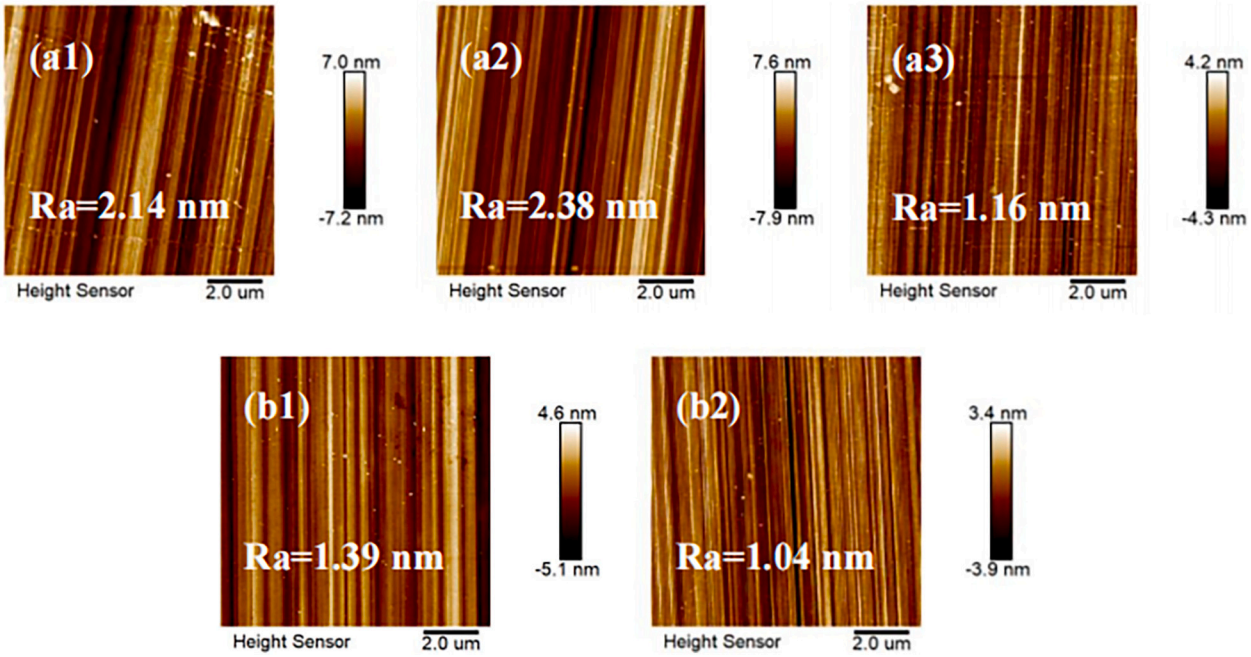

Fig. 2. AFM images of diamond surface. (a1). SCD1 initial surface, (a2). SCD1 plasma etched surface, (a3). SCD1 polished surface, (b1). SCD5 initial surface, (b2). SCD5 polished surface.

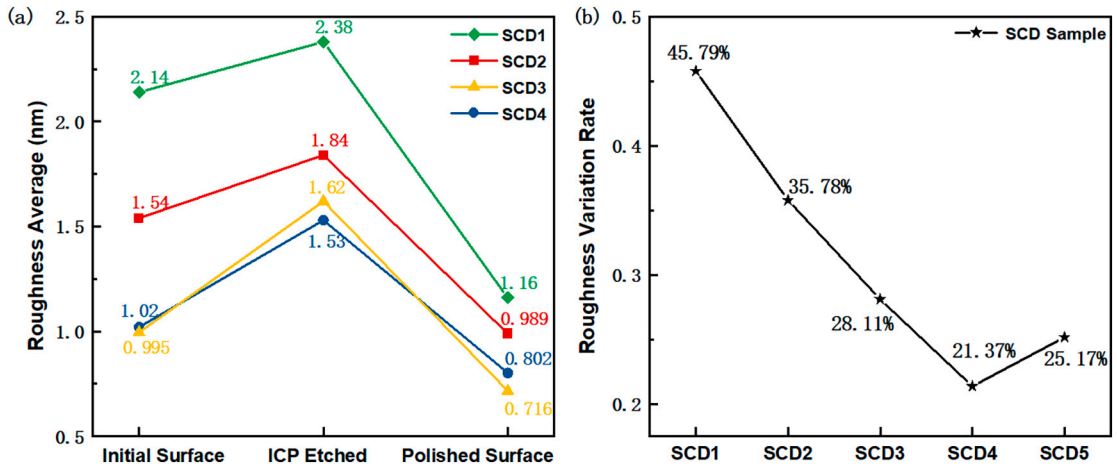

Fig. 3. (a). SCD1, SCD2, SCD3 and SCD4 roughness variation curves, (b). SCD1, SCD2, SCD3, SCD4 and SCD5 roughness variation rate curves.

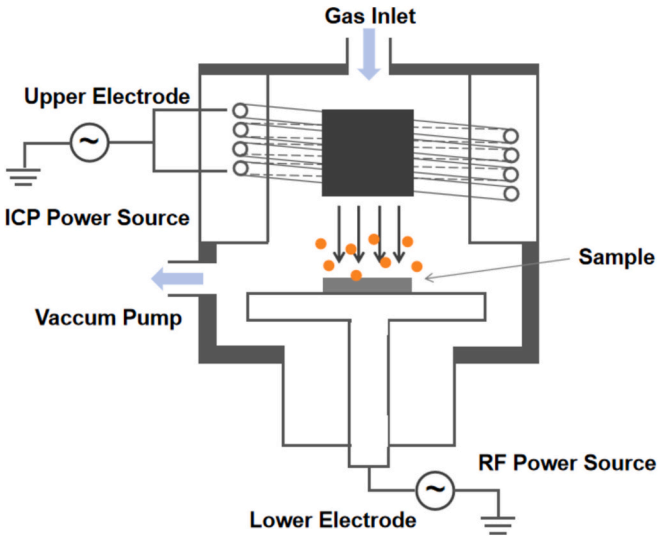

Fig. 4. Schematic diagram of ICP plasma etching system.

3. Results and discussion

3.1. AFM characterization

To explore the changes of diamond surface roughness in each experimental stage, AFM was used to characterize the sample surface of each experimental group under a scanning area of 10 μm*10 μm. Fig. 2 shows the AFM schematic diagram of the etched SCD1 and unetched SCD5 sample surfaces. Additionally, to visually represent the changes in surface roughness of SCD1, SCD2, SCD3 and SCD4 during the polishing process, the roughness variation curves for the samples are shown in Fig. 3(a). Fig. 3(b) shows roughness variation rate after polishing compared to initial surface.

Fig. 4 shows the schematic diagram of our ICP plasma etching system. The ICP device has two independent radio frequency power sources, and the upper electrode is connected to the coil will generate an alternating magnetic field inside. Under a sufficiently large field strength, the gas will enter the plasma state, where the uncharged free radicals will produce isotropic chemical reaction etching with the carbon atoms on the diamond surface, resulting in CO, CO_2 and other gases being brought out of the cavity. In addition, the lower electrode inside the cavity will provide energy for charged ions, so that it can vertically bombard the diamond surface under the action of bias voltage, resulting

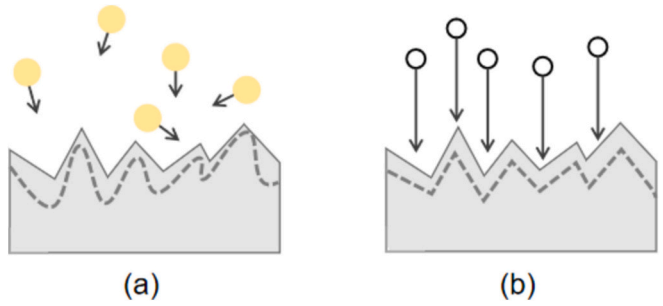

Fig. 5. (a). Surface after isotropic etched, (b). surface after anisotropic etched.

in the action of physical bombardment, anisotropic etching is happened. Both anisotropic etching and isotropic etching jointly lead to the diamond surface changes from orderly to disorderly, the original stable diamond structure is destroyed, and a large number of amorphous carbon composed of sp^2 C and sp^3 C is generated. Since amorphous carbon is unstable, it is easier to be removed by polishing. Fig. 5 shows the schematic diagrams of anisotropic etching and isotropic etching on the diamond surface.

As shown in Fig. 3(a), the roughness of the diamond will increase after ICP etching, which is because the initial surface of the sample has been relatively flat, and although the bombardment of the plasma can cause the protruding part to be carved, the original surface will produce amorphous carbon and other substances, which increases its surface roughness.

By comparing the SCD1 and SCD2, it can be seen that increasing the power of the lower electrode to a certain extent increases the physical bombardment of the plasma, which makes the etching of the samples more rough. After ICP etching, the surface roughness increased by 11.2 %, 19.5 % for SCD1 and SCD2, respectively. The stronger bombardment means that the content of amorphous carbon generated by structural damage on the diamond surface is higher. Therefore, for the SCD2 with higher lower electrode power, the content of amorphous carbon is larger after etching. However, the larger lower electrode power will lead to excessive plasma bombardment, which will cause diamond surface to be worse and is not conducive to fast obtain a high quality polished surface.

By comparing the SCD1 and SCD3, increasing the upper electrode power will make the field strength larger, so that more oxygen molecules will enter the plasma state, and the plasma content in the cavity will increase significantly. Therefore, the effect of isotropic chemical reaction and anisotropic physical bombardment will increase. The surface roughness increased by 62.8 % for SCD3 after ICP etching. More plasma is involved in the reaction of carbon atoms on the diamond surface, this

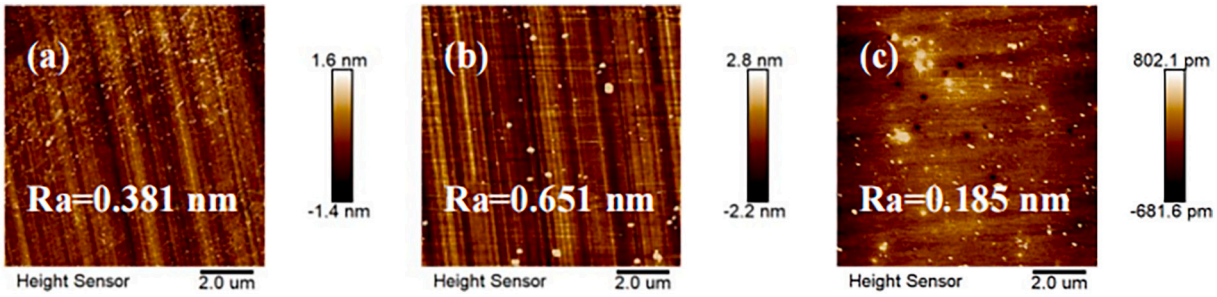

Fig. 6. AFM images of SD6 diamond surface. (a). initial surface, (b). etched surface, (c). polished surface.

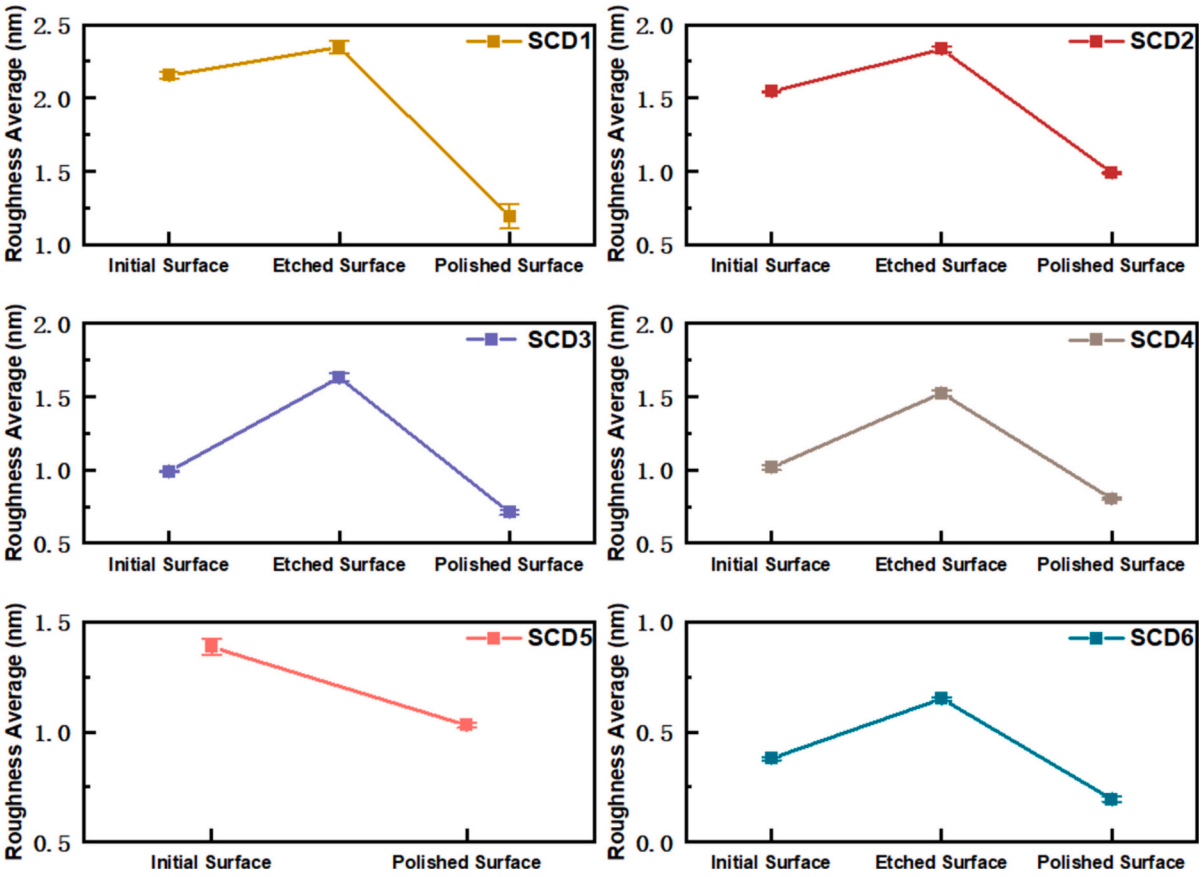

Fig. 7. Diamond surface roughness error bar.

will also cause excessive etching on relatively flat surfaces, so both the etched and polished surfaces are worse than that of the SCD1 sample.

For SCD1 and SCD4, increasing the etching time increases the time of the plasma action on the surface of the sample. However, the long etching time also causes the worse surface after ICP etching. In most cases, the diamond surface etched by ICP has a higher polishing efficiency. However, the roughness variation rate of SCD4 is 21.37 %, which is lower than that of unetched SCD5. In Fig. 3(b), by comparing roughness variation rate of each sample after polishing, SCD1 shows the optimal value. This suggests that the proper etching parameters, such as controlling the power of the upper and lower electrodes and the etching time, are necessary to obtaining a higher quality diamond surface.

Moreover, to explore whether this experimental method can further polish the smooth SCD surface to lower roughness, and the effects on the speed of the platform in the DFP polishing experiment on the polishing experiment, another control group with very low surface roughness and a polishing speed of 70 rpm was set as SCD6, and the remaining experimental parameters were the same as those in the SCD1 experimental group. Fig. 6 shows the AFM schematic diagram of the SCD6.

From the SCD1 and SCD6, it can be seen that increasing the polishing speed will make the amorphous carbon that generated during the etching process and polishing process be removed faster. Finally, Ra value as low as 0.185 nm was achieved after 8 h polishing which is much better than the typical value of 0.42 nm [16]. And the roughness variation rate of SCD6 is 51.44 %.

To reflect the variability and statistical significance, the surface roughness of each sample has been tested at least three times. The error bars are shown in Fig. 7.

3.2. *Raman spectrum analysis*

To further evaluate the crystal structure of SCD after ICP etching and DFP treatment and the change of amorphous carbon content in each experimental stage, Raman spectrum was introduced. It is a technique

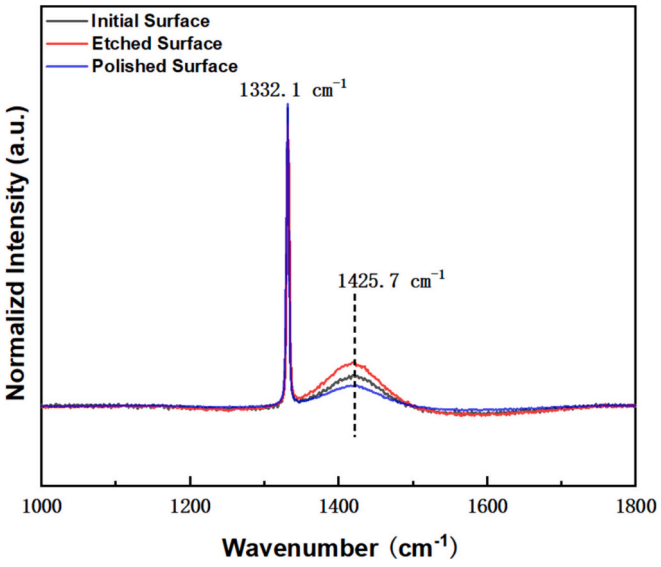

Fig. 8. SCD6 normalized Raman spectra.

with high sensitivity for characterizing different forms of carbon materials [17,18]. The standard characteristic peak of diamond is 1332 cm^{-1} [19], and the Raman displacement at 1580 cm^{-1} corresponding to the G-peak of sp^2 graphite phase. Therefore, there is generally a weak and wide peak at 1425 cm^{-1}, which is the amorphous carbon peak [20] composed of sp^3 C and sp^2 C. In this study, the Raman spectral sample measurement was performed under the laser light source of 532 nm. Fig. 8 shows the normalized Raman spectrum chart of SCD6 samples at each experimental stage.

It can be seen from the comparison of Raman spectrum in each stages that after a period of etching, the amorphous carbon content of the diamond sample at the peak position of 1425 cm^{-1} is higher than the initial state, while after subsequent polishing treatment, the amorphous carbon content is reduced to the lowest level, which is in line with the production and deposition of amorphous carbon caused by the plasma bombardment mentioned above. And finally the mechanism of removing by polishing. In addition, by comparing the sharp characteristic peaks of the diamond in the three stages, the peak position does not shift. Thus, the diamond sample does not undergo chemical deterioration during the experiment.

3.3. XPS peak fitting test

XPS was used to determine the structure and chemical bond evolution of the diamond sample surfaces at each stage of the experiment. In this study, the C 1 s and O 1 s peaks of the SCD6 sample group were tested by XPS, and diamond C—C peaks with an energy of 284.80 eV were calibrated. All peak fitting was carried out in “advantage” software, as shown in Figs. 9 and 10. In Fig. 9(b), it is observed that C 1 s peaks at 283.46 eV and 284.80 eV are mainly disentangled into two components, which belong to sp^2 graphite phase [21] and sp^3 diamond phase [22] respectively. Fig. 10 shows the peak of O 1 s [23,24] at 531.82 eV and 532.01 eV is decomposed into two components, among which the peak at 531.82 eV belongs to the C-O-C bond.

The values in Table 2. represent the peak area of the XPS peak

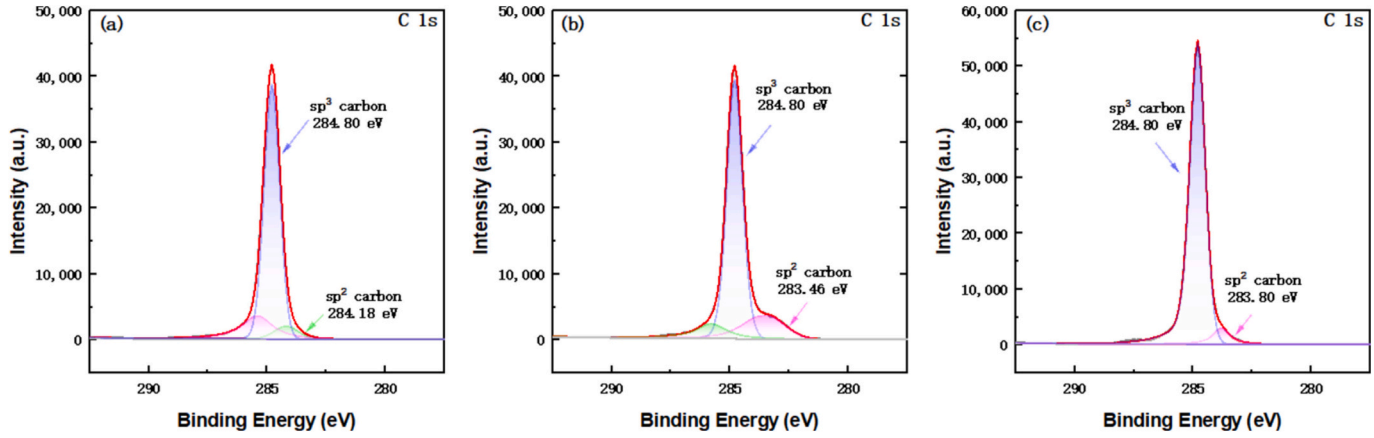

Fig. 9. Fine fitted C 1 s XPS spectra of SCD6. (a). initial surface, (b). etched surface, (c). polished surface.

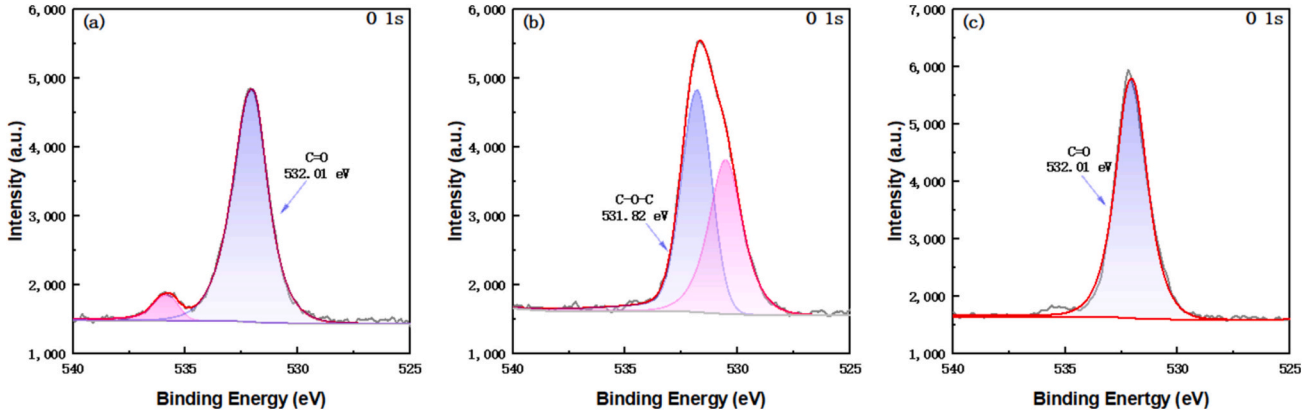

Fig. 10. Fine fitted O 1 s XPS spectra of SCD6. (a). initial surface, (b). etched surface, (c). polished surface.

Table 2
The content changes of C-O-C bond, sp^2 graphite phase and sp^3 diamond phase in XPS spectra before and after ICP etching.

Peak area	Initial surface	Plasma etched surface	Polished surface
Sp^3 diamond phase	33,062.60	33,579.81	48,392.1
Sp^2 graphite phase	2513.96	8188.70	3565.65
C-O-C bond		4772.55	

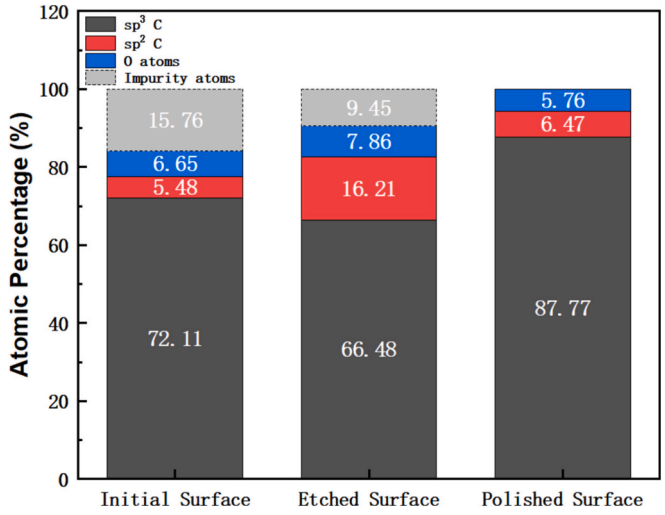

Fig. 11. The percentage of sp^2 C, sp^3 C and O atoms on the surface of the three stages of the SCD6 sample.

obtained by fitting, and the peak area represents the atomic content of sp^3 C, sp^2 C, and C-O-C bond on the diamond surface at each stage, which is a relative value without a specific unit. From the C 1 s peak fitting diagram and atomic content table, it can be seen that at the beginning of the experiment, there is a small amount of sp^2 graphite phase on the diamond surface, and after ICP etching, the peak strength of sp^2 C at 283.46 eV increases significantly. Because amorphous carbon is a mixture of sp^2 C and sp^3 C. Therefore, the results show that a large amount of amorphous carbon is produced on the diamond surface after plasma etching. While the carbon content of sp^2 in 283.80 eV is significantly reduced after DFP polishing experiment, which indicates that the amorphous carbon generated on the diamond surface has been removed; the peak fitting results of O 1 s also prove that after ICP etching, oxygen atoms mainly exist on the diamond sample in the form of C-O-C bond, and finally can be removed by polishing. The above results are in good agreement with the Raman spectrum test results.

Fig. 11 shows the variation curves of sp^2 C, sp^3 C and O atom content in each experimental stage of SCD6 sample. And the "impurity atoms" are O-F_X and some metal carbonates. It can be seen from the graph that the C atom on the initial surface of SCD6 mainly exists in the form of sp^3 C, which atomic proportion is about 72.11 % of the total atomic amount. After etching by oxygen plasma, the content of O atom increases rapidly from 6.65 % to 7.86 %, in which C-O-C bond accounts for 55.75 % of the total O atom, and the proportion of sp^2 C in C atom also increases from 5.87 % to 17.59 % in the initial surface, which is consistent with the polishing mechanism. After polishing, the content of O atom decreases from 7.86 % of the total atomic amount to 5.76 %, lower than the 6.65 % of the original surface, and the proportion of sp^2 C atom also decreases to 6.86 %, while the content of sp^3 C decreases from the initial 77.25 % to 72.15 % after etching in all C atoms, and finally rises to 93.14 % on the polished surface. From the above data comparison, it can be seen that after plasma etching and polishing, the proportion of sp^3 C content of diamond sample is greatly increased which indicates that the combined application of etching and polishing is extremely important to improve the overall quality of diamond.

4. Conclusions

In this study, we demonstrated a method of combining through ICP etching and DFP for polishing single crystal diamonds. Finally, an extremely low surface roughness of 0.185 nm was achieved. The results of Raman spectrum and XPS peak fitting test confirm that ICP etching can produce amorphous carbon on the diamond surface which can be effectively removed in the subsequent DFP process. This is very effective for improving the polishing effect of diamond. In addition, by improving the upper and lower electrode power of ICP etching, etching time and DFP polishing speed and other experimental parameters, the polishing rate of diamond can be effectively improved, and the polishing process can be further optimized. The above results show that the combination of ICP and DFP is a very promising diamond efficient polishing technology. We expect this technology to make significant contributions to the industrialization of diamond in the future and promote its further application in advanced devices.

CRediT authorship contribution statement

Jiarong Yu: Writing – original draft. **Xinyue Liu:** Writing – review & editing. **Rongbin Xu:** Methodology. **Daquan Yu:** Resources.

Declaration of competing interest

The authors declare that they have no known competing financial interests or personal relationships that could have appeared to influence the work reported in this paper.

Acknowledgments

This work was supported by the National Natural Science Foundation of China under Grant U2241222.

Data availability

Data will be made available on request.

References

[1] T K Doi. Study on high efficiency processing for hard to process material (the 1st report). JSPE Proceedings. (2013). 2013.
[2] R. Otterbach, U. Hilleringmann, Reactive ion etching of CVD-diamond for piezoresistive pressure sensors, Diam. Relat. Mater. 11 (3–6) (2002) 841–844.
[3] J. Philip, P. Hess, T. Feygelson, et al., Elastic, mechanical, and thermal properties of nanocrystalline diamond films, J. Appl. Phys. 93 (4) (2003) 2164–2171.
[4] X. Yuan, Y. Zheng, X. Zhu, et al., Recent progress in diamond-based MOSFETs, Int. J. Miner. Metall. Mater. 26 (2019) 1195–1205.
[5] P.J. Wellmann, Power electronic semiconductor materials for automotive and energy saving applications–SiC, GaN, Ga2O3, and diamond, Z. Anorg. Allg. Chem. 643 (21) (2017) 1312–1322.
[6] M. Thumm, Progress on gyrotrons for ITER and future thermonuclear fusion reactors, Ieee T Plasma Sci. 39 (4) (2010) 971–979.
[7] A.J. Maclean, R.B. Birch, P.W. Roth, et al., Limits on efficiency and power scaling in semiconductor disk lasers with diamond heatspreaders, J. Opt. Soc. Am. B 26 (12) (2009) 2228–2236.
[8] Q. Huang, D. Yu, B. Xu, et al., Nanotwinned diamond with unprecedented hardness and stability, Nature 510 (7504) (2014) 250–253.
[9] G. Yan, Y. Wu, D. Cristea, et al., Mechanical properties and wear behavior of multi-layer diamond films deposited by hot-filament chemical vapor deposition, Appl. Surf. Sci. 494 (2019) 401–411.
[10] J. Watanabe, M. Touge, T. Sakamoto, Ultraviolet-irradiated precision polishing of diamond and its related materials, Diam. Relat. Mater. 39 (2013) 14–19.
[11] P.G. Second, Diamond technology production methods for diamond and gem stones, Nature 1 (1955) 75.
[12] C.D. Ollison, W.D. Brown, A.P. Malshe, et al., A comparison of mechanical lap** versus chemical-assisted mechanical polishing and planarization of chemical vapor deposited (CVD) diamond, Diam. Relat. Mater. 8 (6) (1999) 1083–1090.
[13] Y Zheng, A E.L. Cumont, et al. Smoothing of single crystal diamond by high-speed three-dimensional dynamic friction polishing: optimization and surface bonds evolution mechanism. Int J Refract Met H. 96 (2021) 105472.

[14] Y. Zheng, J. Liu, R. Zhang, et al., Fast smoothing on diamond surface by inductively coupled plasma reactive ion etching, J. Mater. Res. 35 (2020) 462–472.
[15] G.M.R. Sirineni, H.A. Naseem, A.P. Malshe, et al., Reactive ion etching of diamond as a means of enhancing chemically-assisted mechanical polishing efficiency, Diam. Relat. Mater. 6 (8) (1997) 952–958.
[16] E.L.H. Thomas, G.W. Nelson, S. Mandal, J.S. Foord, O.A. Williams, Chemical mechanical polishing of thin film diamond, Carbon 68 (2014) 473–479.
[17] S. Iqbal, M.S. Rafique, S. Akhtar, et al., A comparative study on finding an effective root for the introduction of hydrogen into microplasma during diamond growth, J. Phys. Chem. Solids 122 (2018) 72–86.
[18] Y. Zheng, H. Ye, R. Thornton, et al., Subsurface cleavage of diamond after high-speed three-dimensional dynamic friction polishing, Diam. Relat. Mater. 101 (2020) 107600.
[19] K. Yamamura, K. Emori, R. Sun, et al., Damage-free highly efficient polishing of single-crystal diamond wafer by plasma-assisted polishing, Crip Ann-Manuf Techn. 67 (1) (2018) 353–356.
[20] M.R. Ammar, N. Galy, J.N. Rouzaud, et al., Characterizing various types of defects in nuclear graphite using Raman scattering: heat treatment, ion irradiation and polishing, Carbon 95 (2015) 364–373.
[21] S. Ferro, M. Dal Colle, A. De Battisti, Chemical surface characterization of electrochemically and thermally oxidized boron-doped diamond film electrodes, Carbon 43 (6) (2005) 1191–1203.
[22] K.A.M. Aboua, N. Umehara, H. Kousaka, et al., Effect of mating material and graphitization on wear of aC: H coating in boundary base oil lubrication, Tribol. Lett. 68 (2020) 1–8.
[23] J.M. Werrell, S. Mandal, E.L.H. Thomas, et al., Effect of slurry composition on the chemical mechanical polishing of thin diamond films, Sci. Technol. Adv. Mater. 18 (1) (2017) 654–663.
[24] S. Mandal, E.L.H. Thomas, L. Gines, et al., Redox agent enhanced chemical mechanical polishing of thin film diamond, Carbon 130 (2018) 25–30.